On shear correction factors in the non-linear theory of elastic shells

Jacek Chróścielewski [a], Wojciech Pietraszkiewicz [b], Wojciech Witkowski [a,*]

[a] Gdańsk University of Technology, Faculty of Civil and Environmental Engineering, Department of Structural Mechanics and Bridge Structures, Gdańsk 80 952, Poland
[b] Institute of Fluid-Flow Machinery, PASci, ul. Fiszera 14, 80 952 Gdańsk, Poland

ABSTRACT

Theoretical values of two correction factors $\alpha_s = 5/6$ and $\alpha_t = 7/10$ are established for the respective transverse shear stress resultants and stress couples within the general, dynamically and kinematically exact, six-field theory of elastic shells. These values do not depend on the shell material symmetry, geometry of the base surface, the shell thickness, or any kind of kinematic and/or dynamic constraints. The analysis is based on the complementary energy density following from the transverse shear stresses acting only on the shell cross section. The appropriate quadratic and cubic distributions of the stresses across the thickness allow one to derive the consistent constitutive equations for the transverse shear stress resultants and stress couples with α_s and α_t as the respective correction factors. Four numerical examples of highly non-linear shell structures illustrate the influence of different values of α_s and α_t on the results. In particular, some influence of α_t is noticed on the placement of bifurcation points. In dynamic problem of flight of three intersecting plates analysed with Newmark-type temporal algorithm, the value of α_t influences the moment at which the relative error of total energy of the system begins to grow indefinitely leading to the solution failure.

© 2010 Elsevier Ltd. All rights reserved.

1. Introduction

The general non-linear theory of shells proposed by Reissner (1974) was developed in a number of papers, for example by Libai and Simmonds (1983), Chróścielewski et al. (1992, 1997, 2002), Ibrahimbegović (1997) and Eremeyev and Pietraszkiewicz (2006, 2009), and partly summarised in the books by Libai and Simmonds (1998), Chróścielewski et al. (2004) and Eremeyev and Zubov (2008), where many additional references are given. This dynamically exact and kinematically unique two-dimensional (2D) shell model does not require any kind of kinematic or dynamic constraints. It naturally includes the so-called drilling rotation and two transverse shear stress couples with corresponding work-conjugate transverse shear bendings. These fields become of primary importance in analyses of irregular shells with kinks, branchings and intersections (Chróścielewski et al., 1997, 2004), when connecting shell elements with beams, columns and stiffeners, as well as in two-dimensional formulation of singular phenomena such as phase transitions (Eremeyev and Pietraszkiewicz, 2004, 2009), crack propagations, dislocations (Eremeyev and Zubov, 2008), wave motion etc.

Within the general 6-field shell model used here it is also reasonable (Chróścielewski et al., 1997) to introduce explicitly the shear correction factors α_s and α_t into the constitutive equations for the respective transverse shear stress resultants and stress couples. Yet, the numerical values of α_s and α_t are not established within the general shell model, although one expects that the results should be analogous to those available for simplified shell and plate models of the Timoshenko–Reissner (T–R) type formulated using kinematic and/or dynamic constraints. Please note that various T–R shell models developed in many works and summarized for example by Naghdi (1972), Pietraszkiewicz (1979), Altenbach and Zhilin (1988), Simo and Fox (1989), Kleiber and Woźniak (1991), Antman (1995), Rubin (2000), Bischoff et al. (2004), and used by Vu-Quoc et al. (2000, 2001) and Vu-Quoc and Ebcioglu (2000, 2005) in multilayered shells, is based on kinematic constraints: "*shell material fibres, which are initially normal to the undeformed shell base surface, are constrained to remain straight (and possibly inextensible) during shell deformation*". This leads to only two rotational dofs available in such shell models. The absence of the third drilling rotational dof makes the kinematically constrained shell models insufficient for proper analyses of the irregular shell problems mentioned above.

The aim of this paper is to establish theoretical values of the two shear correction factors within the general 6-fields geometrically non-linear theory of elastic shells, and to test their influence on numerical results of static and dynamic behaviour of some highly non-linear regular and irregular shell structures.

After reminding some general shell relations, we discuss in Section 3 an effective part of 3D complementary energy density of the geometrically non-linear elasticity. This part is associated

---

* Corresponding author. Tel.: +48 58 347 21 47; fax: +48 58 374 16 70.
E-mail address: wojwit@pg.gda.pl (W. Witkowski).

with the transverse shear stress components acting only on the shell cross section. Then 3D distribution of the transverse shear stresses are represented in (1.10) through the transverse shear stress resultants and stress couples. The corresponding distribution functions (1.12) are constructed by requiring four conditions (1.11) to be satisfied. The 3D stress distribution is then introduced into the effective 3D density and the through-the-thickness integration is performed. This leads to appropriate forms of the constitutive equations (1.15) and their inverse (1.17). As a result, the uniquely defined theoretical values of the correction factors $\alpha_s = 5/6$ and $\alpha_t = 7/10$ for the respective transverse shear stress resultants and stress couples are established. We refer in Section 4 to some review papers, in which various attempts to calculate α_s within the simplified shell models based on kinematic constraints are summarised, and review few earlier attempts to derive the correction factor α_t within the simplified shell models.

In Section 5, we present four numerical examples of highly non-linear behaviour of elastic shell structures. In two first ones the influence of α_s and α_t on static, stability and post-buckling behaviour of the structures are analysed. In the third example we discuss how three different values of α_t influence the total, potential and kinetic energies of the irregular three-plate structure in its free flight in space. The fourth example shows the influence of values of α_s and α_t on numerical results for the shell of variable thickness.

2. Some shell relations

Let $P \subset M$ and $\overline{P} = \chi(P) \subset \overline{M}$ with corresponding edges ∂P and $\partial \overline{P}$ be connected parts of the shell base surface in the undeformed M and deformed $\overline{M} = \chi(M)$ configurations defined by the position vectors $\boldsymbol{x}$ and $\boldsymbol{y}$, respectively, where χ means the deformation. According to Libai and Simmonds (1998) and Chróścielewski et al. (2004) in the referential description the 2D internal stress resultant $\boldsymbol{n}_\nu$ and stress couple $\boldsymbol{m}_\nu$ vectors acting along $\partial \overline{P}$, but measured per unit length of ∂P with the surface outward unit normal vector $\boldsymbol{v}$, are defined by

$$\boldsymbol{n}_\nu = \int_-^+ \boldsymbol{T}\boldsymbol{l}d\xi = \boldsymbol{n}^\alpha \nu_\alpha, \quad \boldsymbol{m}_\nu = \int_-^+ \boldsymbol{z} \times \boldsymbol{T}\boldsymbol{l}d\xi = \boldsymbol{m}^\alpha \nu_\alpha, \quad \int_-^+ \equiv \int_{-h^-}^{+h^+}, \tag{1.1}$$

where $\boldsymbol{T}$ is the 1st Piola–Kirchhoff stress tensor in the shell space, $\boldsymbol{l}$ the unit normal to the reference shell cross section, $\nu_\alpha = \boldsymbol{v} \cdot \boldsymbol{a}_\alpha$, $\alpha = 1, 2$, $\boldsymbol{a}_\alpha$ the surface base vectors of the curvilinear coordinates (ξ_1, ξ_2) on M, ξ the distance from M along the unit normal vector $\boldsymbol{n}$ orienting M such that $\xi \in [-h^-, h^+]$, $h = h^- + h^+$ the shell thickness, and $\boldsymbol{z}$ a deviation vector of the shell material particle in the deformed configuration from $\overline{M}$.

The unique 2D shell kinematics induced by the resultants $\boldsymbol{n}^\alpha$ and $\boldsymbol{m}^\alpha$ consists of the translation vector $\boldsymbol{u}$ and the proper orthogonal (rotation) tensor $\boldsymbol{Q}$, both describing the gross deformation (work-averaged through the thickness) of the shell cross section such that:

$$\boldsymbol{y} = \boldsymbol{x} + \boldsymbol{u}, \quad \boldsymbol{t}_\alpha = \boldsymbol{Q}\boldsymbol{a}_\alpha, \quad \boldsymbol{t} = \boldsymbol{Q}\boldsymbol{n}, \tag{1.2}$$

where $\boldsymbol{t}_\alpha, \boldsymbol{t}$ are three directors attached to any point of $\overline{M}$. As a result, the 2D vectorial stress measures $\boldsymbol{n}^\alpha, \boldsymbol{m}^\alpha$ and the corresponding work-conjugate 2D vectorial strain measures $\boldsymbol{\varepsilon}_\alpha, \boldsymbol{\kappa}_\alpha$ are naturally expressed in components relative to the rotated base $\boldsymbol{t}_\alpha, \boldsymbol{t}$. However, it is usually more convenient to use the material representation of these 2D measures in the form:

$$\mathbf{n}^\alpha = \boldsymbol{Q}^T \boldsymbol{n}^\alpha = \boldsymbol{Q}^T (N^{\alpha\beta}\boldsymbol{t}_\beta + Q^\alpha \boldsymbol{t}) = N^{\alpha\beta}\boldsymbol{a}_\beta + Q^\alpha \boldsymbol{n},$$
$$\mathbf{m}^\alpha = \boldsymbol{Q}^T \boldsymbol{m}^\alpha = \boldsymbol{Q}^T (\boldsymbol{t} \times M^{\alpha\beta}\boldsymbol{t}_\beta + M^\alpha \boldsymbol{t}) = \boldsymbol{n} \times M^{\alpha\beta}\boldsymbol{a}_\beta + M^\alpha \boldsymbol{n}, \tag{1.3}$$

$$\boldsymbol{\varepsilon}_\alpha = \boldsymbol{Q}^T \boldsymbol{\varepsilon}_\alpha = \boldsymbol{Q}^T (\boldsymbol{y}_{,\alpha} - \boldsymbol{t}_\alpha) = \boldsymbol{Q}^T \boldsymbol{u}_{,\alpha} + (\boldsymbol{Q}^T - \boldsymbol{1})\boldsymbol{a}_\alpha = E_{\alpha\beta}\boldsymbol{a}^\beta + E_\alpha \boldsymbol{n},$$
$$\boldsymbol{\kappa}_\alpha = \boldsymbol{Q}^T \boldsymbol{\kappa}_\alpha = \boldsymbol{Q}^T \, \mathrm{ax}(\boldsymbol{Q}_{,\alpha}\boldsymbol{Q}^T) = \mathrm{ax}(\boldsymbol{Q}^T\boldsymbol{Q}_{,\alpha}) = \boldsymbol{n} \times K_{\alpha\beta}\boldsymbol{a}^\beta + K_\alpha \boldsymbol{n}. \tag{1.4}$$

Here $\boldsymbol{1}$ is the metric tensor of the 3D space and ax $(\cdot)$ denotes the axial vector of the skew tensor $(\cdot)$. In particular, in (1.3) and (1.4) the 2D material components $Q^\alpha = \mathbf{n}^\alpha \cdot \boldsymbol{n}$ and $M^\alpha = \mathbf{m}^\alpha \cdot \boldsymbol{n}$ are the transverse shear stress resultants and couples, while the corresponding work-conjugate 2D material components $E_\alpha = \boldsymbol{\varepsilon}_\alpha \cdot \boldsymbol{n}$ and $K_\alpha = \boldsymbol{\kappa}_\alpha \cdot \boldsymbol{n}$ are the transverse shear strains and bendings, respectively.

3. Constitutive equations for 2D transverse shear measures

In the general six-field theory of shells the strain measures (1.4) are defined only on the shell base surface, without any relations to 3D strain measures in the shell space. Hence, the idea of Pietraszkiewicz (1979) to use the 3D strain energy density for establishing the constitutive equations cannot be applied here.

Let S^{ij}, $i = 1, 2, 3$, be 3D components of the 2nd Piola–Kirchhoff stress tensor $\boldsymbol{S} = \boldsymbol{F}^{-1}\boldsymbol{T}$, where $\boldsymbol{F} = \mathrm{Grad}\ \chi$ is the 3D deformation gradient tensor in the shell space. Since in 3D convected coordinates (ξ_α, ξ), see Pietraszkiewicz and Badur (1983), $\boldsymbol{F}^{-1} = \boldsymbol{g}_i \otimes \bar{\boldsymbol{g}}^i$, $\boldsymbol{T} = T^{ij}\bar{\boldsymbol{g}}_i \otimes \boldsymbol{g}_j$, and $\boldsymbol{S} = S^{ij}\boldsymbol{g}_i \otimes \boldsymbol{g}_j$, with $\boldsymbol{g}_i, \boldsymbol{g}^i$ and $\bar{\boldsymbol{g}}_i, \bar{\boldsymbol{g}}^i$ the 3D base vectors of the undeformed and deformed shell space, respectively, we also have $S^{ij} = T^{ij}$, although $\boldsymbol{S} \neq \boldsymbol{T}$. Thus, in terms of 3D components of $\boldsymbol{S}$ the material 2D stress measures Q^α and M^α are defined by

$$Q^\alpha = \int_-^+ \mu S^{\alpha3} d\xi, \quad M^\alpha = \int_-^+ \mu S^{\alpha3} \xi d\xi, \tag{1.5}$$

with $\mu = 1 - 2\xi H + \xi^2 K$, $H = \frac{1}{2}b_\alpha^\alpha$ the mean curvature, $K = \det\left(b_\beta^\alpha\right)$ the Gaussian curvature, and b_β^α the mixed components of the curvature tensor of M.

The 2D shear stress resultants and moments (1.5) are not the same as those defined in any Timoshenko–Reissner type shell model based on kinematic constraints mentioned above. In our definitions (1.5) the complete 3D distribution of shear stresses $S^{\alpha3}$ are integrated through the thickness, while in analogous definitions of any constrained shell theory the stresses in analogous to (1.5) definitions of shear resultants do not contain reactive stresses which are required to maintain the assumed kinematic constraints, see Kleiber and Woźniak (1991) and Antman (1995).

Within 3D geometrically non-linear, homogeneous elastic solids (Green and Zerna, 1968; Gurtin, 1972) the complementary energy density per unit volume of the reference configuration is given by the quadratic expression:

$$W = -\frac{1}{2} K_{ijkl} S^{ij} S^{kl}, \quad K_{ijkl} = K_{jikl} = K_{ijlk} = K_{klij}, \quad S^{ij} = S^{ji}, \tag{1.6}$$

where K_{ijkl} are components of the compliance 4th-order tensor. In particular, for an isotropic elastic solid we have:

$$K_{ijkl} = \frac{1}{2E}\left[(1 + v)(g_{ik}g_{jl} + g_{il}g_{jk}) - 2vg_{ij}g_{kl}\right], \tag{1.7}$$

with E the Young modulus and v the Poisson ratio.

Taking into account symmetries of K_{ijkl} and S^{ij}, the quadratic expression (1.6) can be written as the sum of four separate terms each representing a part of 3D complementary energy density calculated from the stresses $S^{\lambda\mu}$, $S^{\lambda3}(=S^{3\mu})$ and S^{33}. Only the stress components $S^{\lambda\mu}$, $S^{\lambda3}$ act on the shell cross section. The stress components $S^{3\mu} = S^{\mu3}$, S^{33} act on shell surfaces $\xi = \mathrm{const}$ parallel to the base surface M and, while contributing to the effective part of complementary energy density W^{eff}, they should not contribute to the constitutive equations associated with the resultants (1.1). In particular, the part of W^{eff} from the shear stresses $S^{\alpha3}$ alone is given by

$$W_s^{eff} = -2K_{\lambda 3 \mu 3} S^{\lambda 3} S^{\mu 3} = -2 \frac{1}{\mu^2} A_{\alpha 3 \beta 3} \mu_\lambda^\alpha \mu_\mu^\beta \left(\mu S^{\lambda 3} \right) \left(\mu S^{\mu 3} \right),$$

$$A_{\alpha 3 \beta 3} = K_{\alpha 3 \beta 3}|_{\xi = 0}, \tag{1.8}$$

where $\mu_\lambda^\alpha = \delta_\lambda^\alpha - \xi b_\lambda^\alpha$ are the geometric shifters, see Naghdi (1963).

The 2D representation of W_s^{eff} can now be obtained by direct through-the-thickness integration of (1.8):

$$\Sigma_s^{eff} = \int_-^+ \mu W_s^{eff} d\xi. \tag{1.9}$$

Let us assume, for definiteness, the base surface M be the middle surface of the shell in the undeformed configuration, that is $h^- = h^+ = h/2$. Assume also, for simplicity, that there are no surface tangential forces applied at the upper and lower shell faces where $\xi = \pm h/2$, and no body forces applied in the shell space (otherwise these loads would appear explicitly in the 2D constitutive equations, which we would not like). Then the reduction of 3D transverse shear stress field to its 2D statically equivalent resultant force and couple components according to (1.1) means that in the general shell theory $S^{\alpha 3}(\xi)$ can, in fact, be represented by

$$\mu S^{\alpha 3} = \frac{1}{h} Q^\alpha f(\xi) + \frac{6}{h^2} M^\alpha g(\xi), \tag{1.10}$$

where the functions $f(\xi)$ and $g(\xi)$ should satisfy the following conditions (see Badur, 1984, p. 77):

$$f\left(\pm \frac{h}{2}\right) = g\left(\pm \frac{h}{2}\right) = 0 \quad \text{(a)};$$
$$f(-\xi) = f(\xi), \quad g(-\xi) = -g(\xi) \quad \text{(b)};$$
$$\frac{1}{h} \int_-^+ f(\xi) d\xi = 1, \quad \frac{6}{h^2} \int_-^+ g(\xi) d\xi = 0 \quad \text{(c)};$$
$$\frac{1}{h} \int_-^+ f(\xi) \xi d\xi = 0, \quad \frac{6}{h^2} \int_-^+ g(\xi) \xi d\xi = 1 \quad \text{(d)}. \tag{1.11}$$

The conditions (1.11) are satisfied, in particular, by the following families of polynomials:

$$f_1(\xi) = \frac{3}{2}\left(1 - \frac{4\xi^2}{h^2}\right), \quad f_2(\xi) = \frac{15}{8}\left(1 - \frac{4\xi^2}{h^2}\right)^2,$$
$$f_3(\xi) = \frac{35}{16}\left(1 - \frac{4\xi^2}{h^2}\right)^3, \ldots$$
$$g_1(\xi) = \frac{5}{h}\xi\left(1 - \frac{4\xi^2}{h^2}\right), \quad g_2(\xi) = \frac{35}{4h}\xi\left(1 - \frac{4\xi^2}{h^2}\right)^2,$$
$$g_3(\xi) = \frac{105}{8h}\xi\left(1 - \frac{4\xi^2}{h^2}\right)^3, \ldots \tag{1.12}$$

Each pair of the polynomials $f_n(\xi)$ and $g_n(\xi)$, $n = 1, 2, 3, \ldots$, assure, in particular, that the representation (1.10) for $\mu S^{\alpha 3}(\xi)$ satisfy the tangential force-free boundary conditions at $\xi = \pm \frac{h}{2}$.

When the shell is homogeneous in the transverse normal direction it is quite natural to choose the simplest functions $f_1(\xi)$ and $g_1(\xi)$ in the representation (1.10), and we will use them in this paper as well. In fact, the function $f_1(\xi)$ was first introduced in the linear bending theory of plates by Reissner (1944), while the function $g_1(\xi)$ was first used by Green et al. (1971) in the linear theory of plates of variable thickness.

In case of multi-layer shells with odd number of layers of the same thickness, higher-order functions (1.12) may become more appropriate, for example $f_2(\xi)$ and $g_2(\xi)$ for three-layer shells, $f_3(\xi)$ and $g_3(\xi)$ for five-layer shells, etc. When layers have different thickness and/or their number is even, one has to use the continuity conditions at the layer interfaces to define the global shear correction factors for multi-layer shell through the shear

correction factors of individual layers. Such an approach can directly be used in the dynamically exact multi-layer shells proposed recently by Chróścielewski et al. (in press). Its approximate applicability to geometrically exact multi-layer shell models of Vu-Quoc et al. (2000–2005) can be discussed within the errors of the second approximation to the elastic strain energy density of Pietraszkiewicz (1979), see also discussion in Section 4.

The relations (1.8) and (1.12) for $n = 1$ indicate that the integrand in (1.9) becomes an infinite series of the resultants Q^α, M^α, the curvatures H, K, the material parameters, and polynomials of ξ. Thus, let us now assume that the shell is thin, $h/R \ll 1$, so that $\mu \approx 1$, and $\mu_\lambda^\alpha \approx \delta_\lambda^\alpha$. Introducing these approximations together with (1.12), (1.8) and (1.10) into (1.9), and taking into account that:

$$\int_-^+ f_1^2(\xi) d\xi = \frac{6}{5} h, \quad \int_-^+ g_1^2(\xi) d\xi = \frac{10}{21} h, \tag{1.13}$$

we obtain the following result:

$$\Sigma_s^{eff} = -2A_{\alpha 3 \beta 3}\left(\frac{1}{\alpha_s h} Q^\alpha Q^\beta + \frac{12}{\alpha_t h^3} M^\alpha M^\beta\right), \quad \alpha_s = \frac{5}{6}, \quad \alpha_t = \frac{7}{10}. \tag{1.14}$$

The constitutive equations for the 2D strain components E_α and K_α can now be directly calculated differentiating (1.14):

$$E_\alpha = -\frac{\partial \Sigma_s^{eff}}{\partial Q^\alpha} = \frac{4}{\alpha_s h} A_{\alpha 3 \beta 3} Q^\beta, \quad K_\alpha = -\frac{\partial \Sigma_s^{eff}}{\partial M^\alpha} = \frac{48}{\alpha_t h^3} A_{\alpha 3 \beta 3} M^\beta. \tag{1.15}$$

Let L^{ijkl} be 2D components of the 4th-order elasticity tensor which are dual to A_{ijkl} such that:

$$L^{ijkl} A_{klmn} = \frac{1}{2}\left(\delta_m^i \delta_n^j + \delta_n^i \delta_m^j\right), \quad L^{\gamma 3kl} A_{kl\beta 3} = \frac{1}{2}\delta_\beta^\gamma, \quad L^{\gamma 3\alpha 3} A_{\alpha 3 \beta 3} = \frac{1}{4}\delta_\beta^\gamma. \tag{1.16}$$

Then we can invert the constitutive Eq. (1.15) for Q^α and M^α and obtain:

$$Q^\alpha = \alpha_s h L^{\alpha 3 \beta 3} E_\beta, \quad M^\alpha = \alpha_t \frac{h^3}{12} L^{\alpha 3 \beta 3} K_\beta. \tag{1.17}$$

The values $\alpha_s = 5/6$ and $\alpha_t = 7/10$ of the correction factors derived here do not depend on the shell material symmetry, geometry of the base surface, the shell thickness, or any kind of kinematic and/or dynamic constraints so popular in the literature.

In particular, for the homogeneous isotropic elastic material:

$$A_{\alpha 3 \beta 3} = \frac{1}{4G} a_{\alpha\beta}, \quad L^{\alpha 3 \beta 3} = G a^{\alpha\beta}, \quad G = \frac{E}{2(1+v)}, \tag{1.18}$$

so that the energy (1.14) reads:

$$\Sigma_s^{eff} = -\frac{1}{2Gh} a_{\alpha\beta}\left(\frac{1}{\alpha_s} Q^\alpha Q^\beta + \frac{12}{h^2} \frac{1}{\alpha_t} M^\alpha M^\beta\right), \tag{1.19}$$

and the corresponding constitutive equations are:

$$E_\alpha = \frac{1}{\alpha_s} \frac{1}{Gh} a_{\alpha\beta} Q^\beta, \quad K_\alpha = \frac{1}{\alpha_t} \frac{12}{Gh^3} a_{\alpha\beta} M^\beta, \tag{1.20}$$

$$Q^\alpha = \alpha_s Gh a^{\alpha\beta} E_\beta = \frac{1}{2}\alpha_s C(1-v) a^{\alpha\beta} E_\beta, \quad C = \frac{Eh}{1-v^2},$$
$$M^\alpha = \alpha_t \frac{Gh^3}{12} a^{\alpha\beta} K_\beta = \frac{1}{2}\alpha_t D(1-v) a^{\alpha\beta} K_\beta, \quad D = \frac{Eh^3}{12(1-v^2)}. \tag{1.21}$$

Please note some symmetry of so defined α_s and α_t with regard to the shell stretching and bending stiffness C and D, respectively.

4. Discussion

Since the role of α_t was not understood within the general six-field theory of elastic shells, Chróścielewski et al. (2004) and Chróścielewski and Witkowski (2010a) performed extensive numerical tests in order to analyse how values of α_t influence the static and dynamic behaviour of several regular and irregular elastic shell structures within the linear and geometrically non-linear range of deformation. It was found, in particular, that when $\alpha_t < 1$ the results were practically insensitive to its numerical value. This corresponds well with quantitative estimates provided by John (1965) that in thin shells the order of transverse shear stresses $S^{\alpha 3}$ is lower by some small parameter than the order of stresses $S^{\alpha \beta}$. Thus, the shell complementary energy density following from terms involving Q^α and M^α is of higher-order smallness than the one following from those involving $N^{\alpha\beta}$ and $M^{\alpha\beta}$.

In most plate and shell models available in the literature the shell kinematics, not dynamics as in the present paper, is taken as the primitive notion to which various simplifying kinematic and/or dynamic constraints are applied. In most cases the 3D translation field $\boldsymbol{v}(\xi)$ in the shell space is approximated by the linear expression, see for example Pietraszkiewicz (1979):

$$\boldsymbol{v}(\xi) \cong \boldsymbol{u} + \xi\boldsymbol{\beta}, \quad \boldsymbol{\beta} = \bar{\boldsymbol{a}}_3 - \boldsymbol{n}, \quad \bar{\boldsymbol{a}}_3 = \boldsymbol{Gn}, \quad \boldsymbol{G} = \boldsymbol{F}|_{\xi=0}. \tag{1.22}$$

In particular, the transverse shear strain components $\Gamma_{\alpha 3}(\xi)$ of the 3D Green strain tensor $\boldsymbol{\Gamma} = \frac{1}{2}(\boldsymbol{F}^T\boldsymbol{F} - \boldsymbol{1})$ are approximated by

$$\Gamma_{\alpha 3}(\xi) \cong \gamma_{\alpha 3} + \xi\frac{1}{2}\kappa_{\alpha 3}, \quad \gamma_{\alpha 3} = \frac{1}{2}\bar{\boldsymbol{a}}_\alpha \cdot \bar{\boldsymbol{a}}_3, \quad \kappa_{\alpha 3} = \bar{\boldsymbol{a}}_{3,\alpha} \cdot \bar{\boldsymbol{a}}_3, \quad \bar{\boldsymbol{a}}_\alpha = \boldsymbol{Ga}_\alpha. \tag{1.23}$$

The linear approximations (1.22) and (1.23) are used, for example, in the Timoshenko–Reissner type plate and shell models, geometrically exact formulations, shell models obtained by degeneration of 3D relations, and the 2D models of Cosserat surface with one deformable director. Frequently, in such 2D models the dynamic constraint about the plane stress state in the shell space is additionally assumed. However, the errors introduced into the 2D theory of shells by such kinematic and/or dynamic constraints are not well understood even today.

In all 2D plate and shell models based on such kinematic constraints deformation of the base surface is described only by 5 displacemental degrees of freedoms (dof): three translations and two rotational parameters. The third rotational dof – the so-called drilling rotation – cannot be properly defined here, see extensive discussion of this issue in Chróścielewski et al. (2004), Section 2.7. In order to apply such constrained 2D plate and shell models in analyses of irregular shell problems mentioned in Section 1, one has to additionally reintroduce the drilling dof into the shell relations.

The correction factor $\alpha_s = 5/6$ in the constitutive equations for Q^α expressed in terms of $\gamma_{\alpha 3}$ was first proposed by Bolle (1947) within the linear theory of isotropic elastic plates. He used the quadratic distribution of transverse shear stresses across the plate thickness similar to our (1.10) and (1.12)$_1$. In many later papers reviewed by Grigoljuk and Selezov (1973), Noor and Burton (1989), and Jemielita (2001) various static, kinematic and dynamic approaches were proposed to redefine this factor leading to its different values from the range [0.73–1.0]. In those papers the influence of existence of the transverse shear stress couples M^α on the value of α_s was not taken into account.

The correction factor 7/20 in the constitutive equations for $M^{\alpha 3} \equiv M^\alpha$ was first proposed by Green et al. (1971), see also Naghdi (1972), within the linear theory of isotropic elastic plates of variable thickness. Their work-conjugate bending measures $\rho_{3\alpha}$ were defined as linear combinations of the main $\gamma_{\alpha 3}$ and linear $\kappa_{\alpha 3}$ terms of through-the-thickness expansion of $2\Gamma_{\alpha 3}(\xi)$.

Pietraszkiewicz (1979a) arrived at the correction factors $k^2 \equiv \alpha_s = 5/6$ and $l^2 \equiv \alpha_t = 7/10$, with detailed derivation of these values available in PhD dissertation of Badur (1984). The constitutive equations for $N^{\alpha 3} \equiv Q^\alpha$ and $M^{\alpha 3} \equiv M^\alpha$ in terms of corresponding $\gamma_{\alpha 3}$ and $\kappa_{\alpha 3}$ were derived by Pietraszkiewicz (1979a,b), within the consistent second approximation to the elastic strain energy density of the geometrically non-linear isotropic shells. Comparing those constitutive equations with ours (1.17) we can conclude that within the error indicated in Pietraszkiewicz (1979a,b) the 2D strain measures $2\gamma_{\alpha 3},\kappa_{\alpha 3}$ defined by Pietraszkiewicz (1979a) and in (1.23) can be interpreted as some approximations to E_α, K_α defined in (1.4). However, the both 2D transverse shear strains and bendings should not be identified, because they are introduced by entirely different approaches.

Yeh and Chen (1993) used the transverse shear correction factor $1/\varphi$ with $\varphi = 1.2$ in their micropolar elastic constant matrix of an isotropic plane stress state for both the stress resultants $N^{\alpha 3}$ and stress couples $M^{\alpha 3}$. This corresponds to the assumption that both $\alpha_s = \alpha_t = 5/6$, and such a choice was referred to Owen and Hinton (1980).

Bischoff and Ramm (2000) and Bischoff et al. (2004) used the correction factors $\alpha = 5/6$ and $\beta = 7/10$ in their constitutive equations for $n^{\alpha 3} \equiv Q^\alpha$ and $m^{\alpha 3} \equiv M^\alpha$ within the 7-parameter shell model, while derivation of such factors was referred to Bischoff (1999). The main term of through-the-thickness expansion of the 3D Green strains $E_{\alpha 3}(\xi)$ was $\alpha_{\alpha 3} \equiv \gamma_{\alpha 3}$ while the linear term was denoted as $\beta_{\alpha 3}$, so that $2\beta_{\alpha 3}$ is identical to $\kappa_{\alpha 3}$ given in (1.23). Likewise, the measures E_α and $2\varepsilon_{\alpha 3}$ as well as K_α and $2\beta_{\alpha 3}$ may be seen as some approximations of each other, but they should not be identified.

Altenbach and Eremeyev (2009) suggested that the constitutive relations used in the general shell theory may be viewed as equivalent to their material law proposed for the Cosserat plates. In particular, Chróścielewski and Witkowski (2010a) derived from results of Altenbach and Eremeyev (2009) the analytic formula for α_t valid in the case of non-polar material:

$$\alpha_t = \frac{2 - v}{1 - v}. \tag{1.24}$$

Since such $\alpha_t \geqslant 2$ for any $1 > v \geqslant 0$, it seems that the constitutive equations for Q^α was derived by Altenbach and Eremeyev (2009) using different 2D bending measure not compatible with our K_α.

This discussion explicitly indicates that α_t is the constitutive coefficient which must not be confused with a 'penalty multiplier' as it was used in Eberlein and Wriggers (1999) and Tan and Vu-Quoc (2005).

The discussion above also indicates that the values $\alpha_s = 5/6$ and $\alpha_t = 7/10$ of the correction factors derived here can also be used with good approximation in any geometrically non-linear versions of homogeneous elastic plates and shells formulated by applying various simplifying kinematic constraints of Timoshenko–Reissner type leading to 5, 6 or 7-parameter models, geometrically exact formulations, 2D models degenerated from 3D elasticity, Cosserat surface models with one deformable director, etc. This is so, because according to John (1965) the stresses $S^{\alpha 3}$ in the shell space are of lower order than those of $S^{\alpha\beta}$. Hence, the energy introduced by Q^α and M^α themselves into the 2D complementary energy density of the shell is small, and eventual additional errors of kinematic constraints on the values of shear correction factors is expected to be of higher-order smallness.

5. Numerical examples

The remainder of this paper is concerned with numerical examples that study influence of the values of α_s and α_t on the response of shell structures in FEM analysis. In numerical results

to follow we use the 16-node displacement/rotation based elements CAMe16 with full integration of element matrices, see Chróścielewski et al. (1992, 2004). Using dense meshes we avoid discussions about locking phenomena and convergence. The analysis is performed within small elastic strains but unlimited translations and rotations.

5.1. Static snap-through of cylindrical panel

Consider a cylindrical panel depicted in Fig. 1, where the geometry and boundary conditions are shown. The material parameters are $E = 2 \times 10^{11}$, $v = 0.25$, $h = 0.01$. This example was examined, among others, in Botasso et al. (2002), Kuhl and Ramm (1996) to study properties of time integration schemes. Here we are concerned with the static version of this example.

In the first part we have studied one quarter of the panel due to the double symmetry. At the first stage we have performed mesh convergence analysis for two discretisations of the quarter with 8×8 and 12×12 CAMe16 elements. It turns out that there has been no significant difference in the results, so we present only the results obtained in the first mesh.

In the second part we have studied the influence of different values of α_t. The overall response of the structure has been almost indistinguishable for $\alpha_t = 0.01$ and $\alpha_t = 2.33$, with the latter value obtained from (1.24). To show the complicated nature of the analyzed problem Fig. 2 depicts the non-linear load-deformation path of translation w of the point (a), and Fig. 3 shows the path of translation u for the point (a). To conclude the study on symmetric analysis, Fig. 4 portrays the load–displacements path in the vicinity of the first limit point from Fig. 2. As it can be observed from Fig. 4, the change of $\alpha_t = 0.01$ into $\alpha_t = 2.33$ does not practically change the placement of the limit point.

However, the value of α_t has some influence on the non-symmetric bifurcation point. Fig. 5 shows the placements of
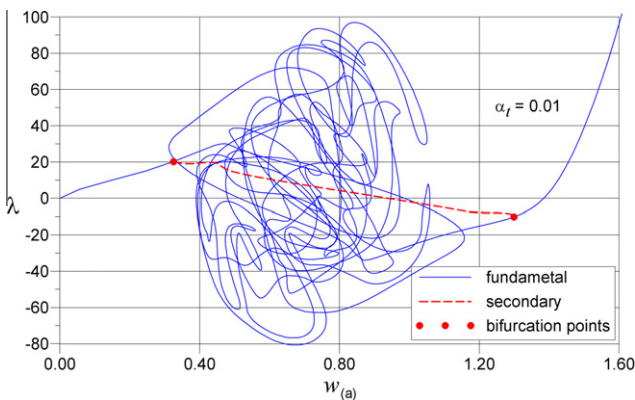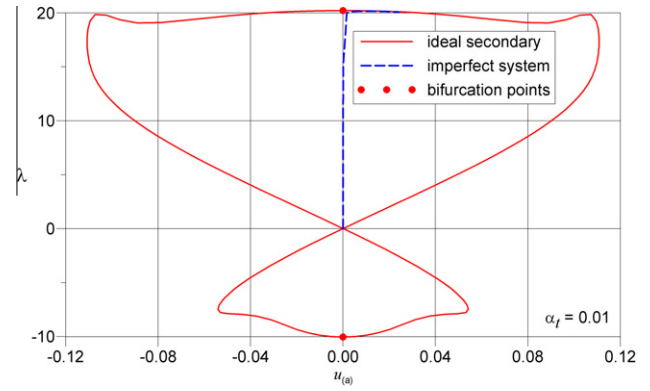

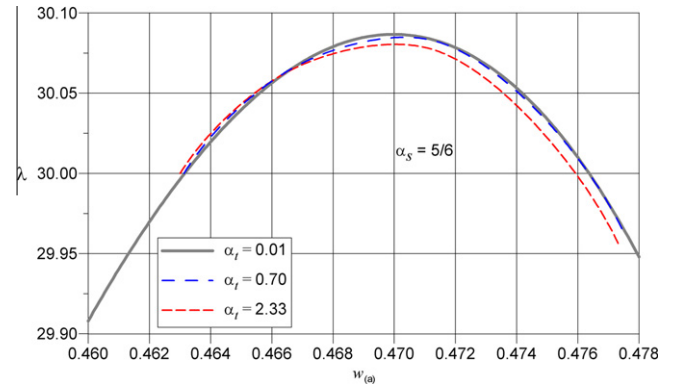**Fig. 3.** Cylindrical shell: load-deformation path of $u_{(a)}$.

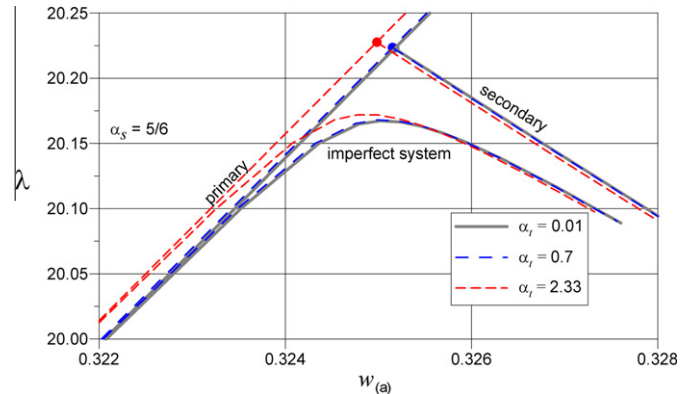**Fig. 4.** Cylindrical shell: vicinity of the first limit point, symmetry.

Fig. 5. Non-linear deformation path, bifurcation point.

bifurcation points depending on α_t. While for $\alpha_t = 0.01$ and $\alpha_t = 0.7$ the response of the structure is almost the same, for $\alpha_t = 2.33$ the bifurcation occurs for slightly larger value of the control parameter λ.

Finally, Figs. 6 and 7 depict placements of the upper and lower limit points from Fig. 3, respectively.

The presented results show small influence of the value of α_t on the obtained results. The only exception is the placement of the bifurcation point in the case of asymmetric buckling.

5.2. Channel section cantilever

The problem analyzed in this subsection was originally formulated by Lee and Haris (1979) as the simply supported beam

Fig. 1. Cylindrical shell: geometry, load and boundary conditions.

Fig. 2. Cylindrical shell: load-deformation path of $w_{(a)}$.
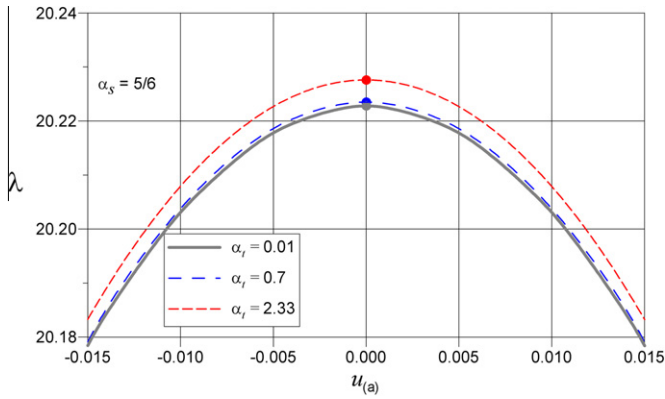
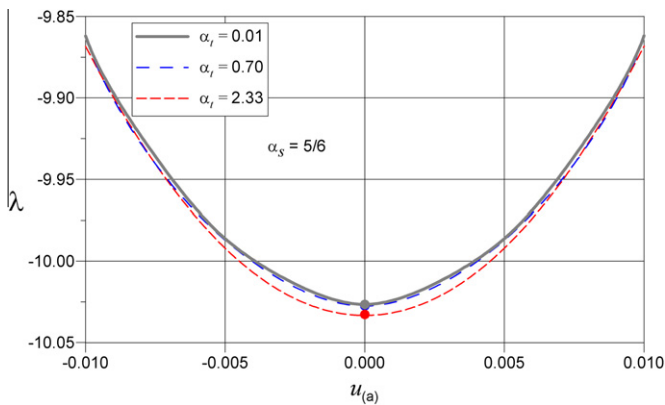Fig. 6. Upper bifurcation point on secondary path.

Fig. 7. Lower bifurcation point on secondary path.

under action of uniformly distributed transverse load. Later, Chróścielewski et al. (1992) analyzed another variant of this example: the beam was considered as clamped at one end with the point load applied at the free end. This version became the popular benchmark problem and was analyzed among others by Ibrahimbegović and Frey (1994), Betsh et al. (1996), Chróścielewski et al. (2004), Eberlein and Wriggers (1999), Tan and Vu-Quoc (2005). Wagner and Gruttmann (2005) studied another variant of this example, see also Chróścielewski and Witkowski (2006).

The structure analysed here is depicted in Fig. 8. Geometry is described by $L = 36$, $a = 2$, $b = 6$, $h = 0.05$ while the load is assumed as proportional $P(\lambda) = \lambda P_{ref}$ with $P_{ref} = 100$. The material constants are $E = 10^7$ and $v = 0.333$. The mesh used in this study consists of 4 elements for lower flange, 6 elements for the web, 4 elements for the upper flange and 36 elements along the beam length. Fig. 9 portrays non-linear load-deformation path of the horizontal
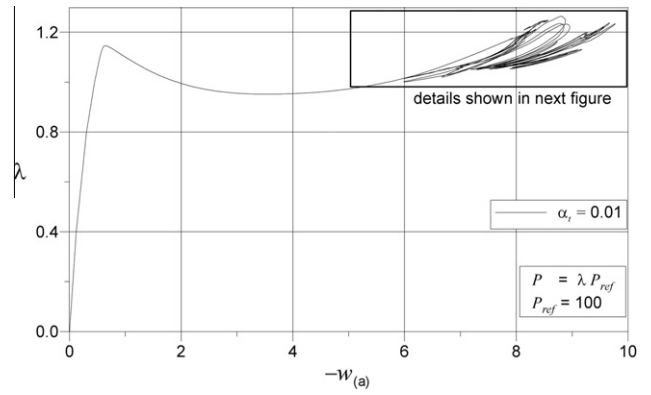

Fig. 9. Channel section cantilever: non-linear deformation paths.

translation w of the point (a) obtained using $\alpha_t = 0.01$. As it can be seen, the response of the structure is complex for values $w > -6$. Fig. 10 shows the non-linear deformation paths of w obtained with three different values of $\alpha_t = [0.01; 0.7; 2.499]$. The latter value is obtained based on Eq. (1.24). It may be noted that all the solutions are close to each other. This Figure also shows the complicated response of the structure. Details of this response are shown in Fig. 10.

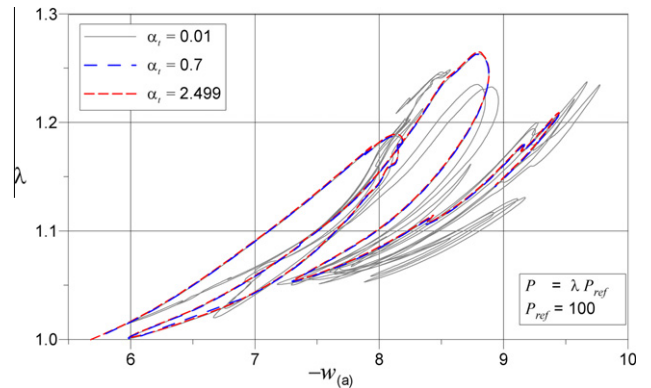Similarly to the previous example, numerical results show small dependence on the values of α_t.

Fig. 10. Channel section cantilever: non-linear deformation paths, details.

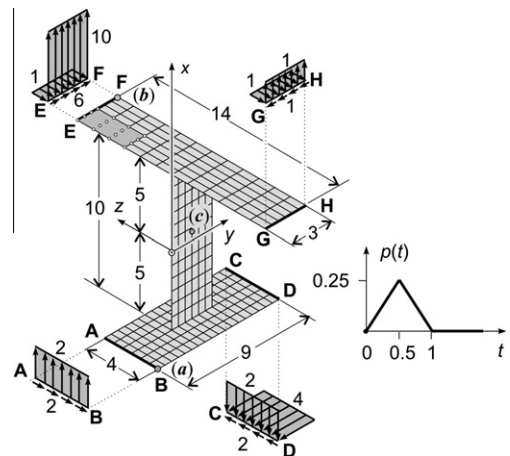Fig. 8. Channel section cantilever: geometry and load.

Fig. 11. Three intersecting plates: geometry and loads.

5.3. Free flight of three intersecting plates

This example is representative for the class of tumbling problems initiated by the works of Vu-Quoc and Simo, see Vu-Quoc (1986), Simo and Vu-Quoc (1988). We analyze the flight of the shell structure as shown in Fig. 11, where geometry, loads and material parameters are given. This example was analyzed by Simo and Tarnow (1994), Zhong and Crisfield (1998), Miehe and Shroeder (2001). It is interesting to notice that Miehe and Shroeder (2001) and Simo and Tarnow (1994) obtained different results though the same material, loads and geometrical parameters were used. This issue has recently been studied in detail by Chróścielewski and Witkowski (2010a), where the internal, kinetic and total energies, the kinetic constitutive equations and the time integration schemes were described. The importance of this example is that once the external load impulse dies out in free motion the structure is the Hamiltonian system in which we observe, conserved by definition, the total energy of the structure.

The material constants in used in this example are $E = 2 \times 10^7$, $v = 0.25$, $h = 0.02$.

Simulations carried out in this paper are based on the kinetic constitutive relations for the linear $\boldsymbol{p}(\boldsymbol{x},\boldsymbol{t}) = \rho_m h \boldsymbol{v}$ and angular $\boldsymbol{j}(\boldsymbol{x},t) = (\rho_I h^3/12)\boldsymbol{\omega}$ momentum vectors in which $\boldsymbol{v} = \dot{\boldsymbol{y}}(\boldsymbol{x},t) = \dot{\boldsymbol{u}}(\boldsymbol{x},t)$ and $\boldsymbol{\omega} = ax(\dot{\boldsymbol{Q}}\boldsymbol{Q}^T)$ are the translational and angular velocity vectors, and coefficients are given by

$$\rho_m h = 1.0 \cdot 0.02 = 0.02, \quad \rho_I \frac{h^3}{12} = 50 \cdot \frac{0.02^3}{12} = 3.333 \times 10^{-5},$$

$$(1.25)$$

where ρ_m stands for the initial mass density of the translational motion, and ρ_I is the initial mass density of the rotary motion.

In this example we have used two time integration schemes. The first one belongs to the Newmark family and was described in Chróścielewski et al. (2004), Lubowiecka and Chróścielewski (2002). The second scheme falls into category of the energy-conserving algorithms (ECA, this label is used in the figures to designate the solutions) and its details were given by Lubowiecka and Chróścielewski (2005).

The ECA algorithm has also been used in the paper by Chróścielewski and Witkowski (2010b). To validate the correctness of the scheme the authors run the example known as the toss rule (see for example Kuhl and Ramm, 1996; Vu-Quoc and Tan, 2003). It has been shown that the present ECA algorithm furnishes correct results.

The time step used in the present calculations has been taken as $\Delta t = 0.002$ s.

Fig. 12 shows preservation of the total energy of the structure obtained for three different values of the correction factor
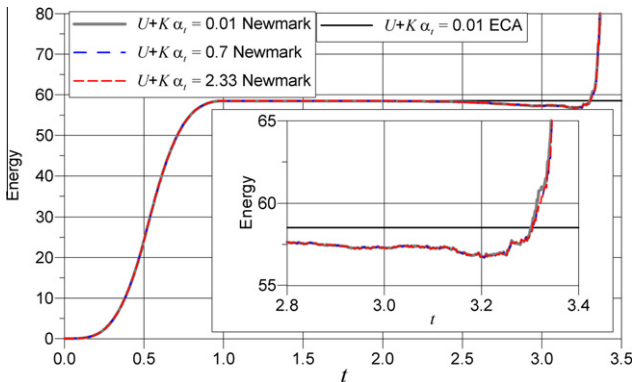
$\alpha_t = [0.01; 0.7; 2.33]$ by making use of the Newmark algorithm. The value $\alpha_t = 2.33$ is obtained through (1.24). These three results are compared to the solution obtained for $\alpha_t = 0.01$ with the ECA method. When $t \approx 3.3$ s we observe a sudden growth of the total energy for all three values of α_t in the Newmark scheme. As it can be observed, for $\alpha_t = 0.01$ this convergence failure appears slightly later than for the two remaining values. The same effect is portrayed in Figs. 13 and 14 for the kinetic K and potential U energies, respectively. To compare the results further we define the relative energy error as

$$\text{error} = 100\% \cdot \frac{U + K - G_{\text{ext}}}{G_{\text{ext}}}, \tag{1.26}$$
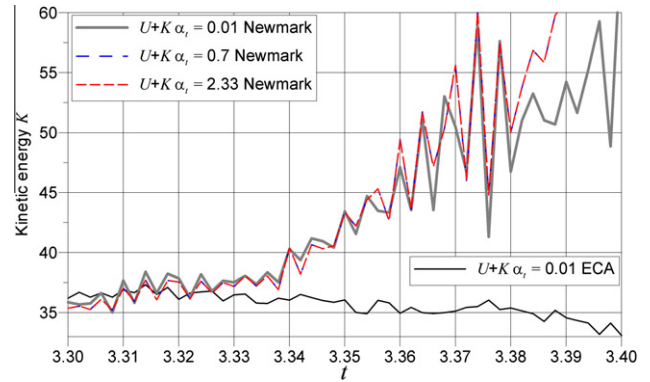

Fig. 13. Three intersecting plates: kinetic energy for different values of α_t.
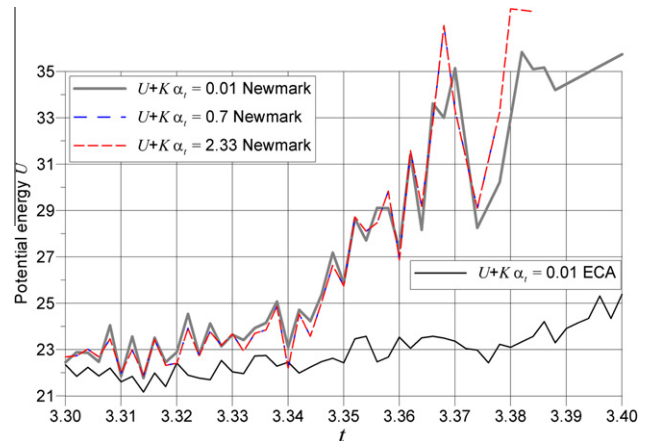

Fig. 14. Three intersecting plates: potential energy for different values of α_t.

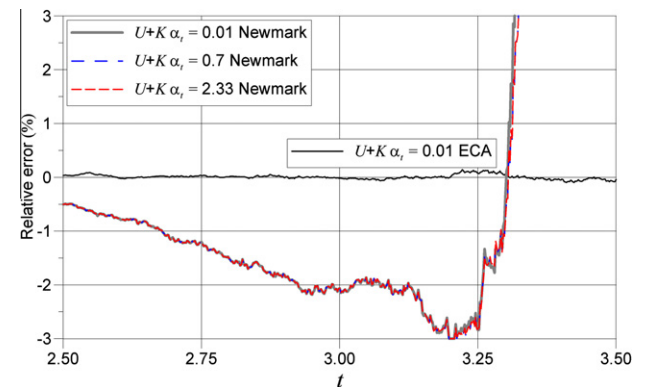**Fig. 12.** Three intersecting plates: total energy for different values of α_t.

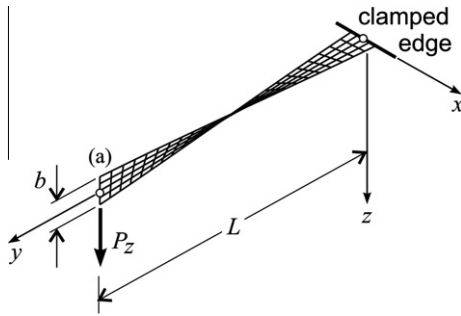**Fig. 15.** Three intersecting plates: relative error of the total energy, Eq. (1.26).

Fig. 16. Twisted beam, geometry and load.

where the external work G_{ext} is defined in Chróścielewski and Witkowski (2010a). The error plotted against time t is shown in Fig. 15.

5.4. Bending of twisted beam

We analyze the twisted beam shown in Fig. 16. This example was used in the set of problems proposed by MacNeal and Harder (1985). Originally, the thickness $h = 0.32$ was used. Belytschko et al. (1989) reduced the thickness to $h = 0.0032$ to invoke the locking effect. This is the very popular example, see for instance Wagner and Gruttmann (2005), Chróścielewski and Witkowski (2006), Panasz and Wiśniewski (2008), Cardoso et al. (2008) and the literature given there. In computations we use the following data: $L = 12$, $b = 1.1$, angle of twist 90°, $E = 29 \times 10^6$, $v = 0.22$. We perform the analysis for three different values of thickness:
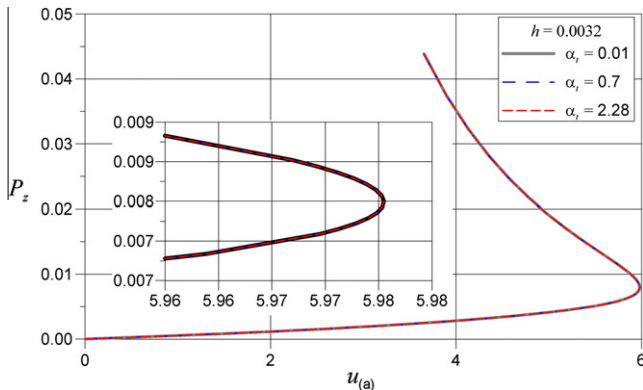

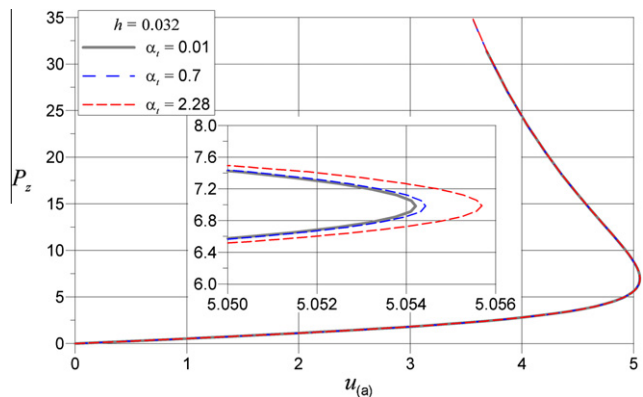**Fig. 17.** Twisted beam, results for $h = 0.0032$.

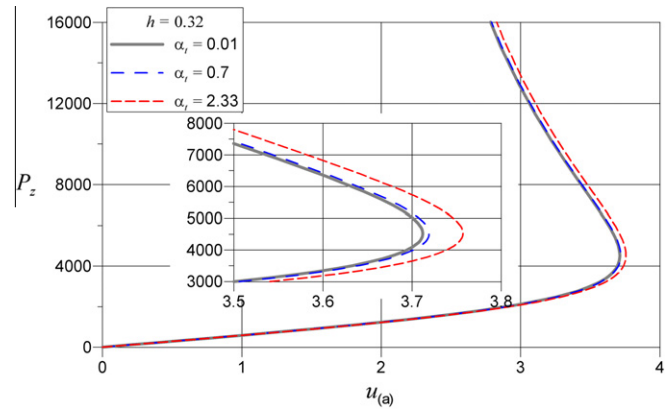**Fig. 18.** Twisted beam, results for $h = 0.032$.

Fig. 19. Twisted beam, results for $h = 0.32$.

$h = 0.32$, $h = 0.032$, $h = 0.0032$, using three different values of $\alpha_t = [0.01; 0.7; 2.28]$. Here the latter value $\alpha_t = 2.28$ is obtained from (1.24). The results are shown in Figs. 17–19. From the figures it is seen that regardless of the value of α_t the overall response of the structure has the same character. However, with the growth of the shell thickness the influence of α_t becomes more clearly pronounced.

6. Conclusions

We have established the theoretical values of two correction factors $\alpha_s = 5/6$ and $\alpha_t = 7/10$ for the respective transverse shear stress resultants and stress couples within the general, dynamically exact and kinematically unique, six-field theory of elastic shells. This values do not depend on the shell material symmetry, geometry of the base surface, the shell thickness, or any kind of kinematic and/or dynamic constraints.

We have formulated the 2D constitutive equations for the transverse shear stress resultants and stress couples and compared them with those known in the literature, which were obtained using various simplifying kinematic and/or dynamic constraints.

The constitutive equations derived here have been used to analyse numerically four highly non-linear shell structures, in which the influence of different values of α_t known in the literature on the results are illustrated. In particular, little influence of different values of α_t on limit points of the structures has been noted. However, for the placement of bifurcation points the influence of α_t is noticeable indeed.

In case of shell dynamic problem, when the temporal Newmark-type algorithm fails to converge, the value of α_t influences the moment at which the relative error of total energy of the system begins to grow indefinitely leading to the solution failure.

References

Altenbach, H., Eremeyev, V.A., 2009. On the linear theory of micropolar plates. Z. Angew. Math. Mech. 89 (4), 242–256.
Altenbach, H., Zhilin, P.A., 1988. General theory of elastic simple shells. Adv. Mech. 11 (4), 107–148 (in Russian).
Antman, S.S., 1995. Nonlinear Problems of Elasticity. Springer-Verlag, New York, Berlin.
Badur, J., 1984. Non-Linear Analysis of Elastic Shells According to Second Approximation to the Strain Energy (in Polish). Institute of Fluid-Flow Machinery PASci, Gdańsk, Poland.

Belytschko, T., Wong, B.L., Stolarski, H., 1989. Assumed strain stabilization procedure for the 9-node Lagrange shell element. Int. J. Numer. Meth. Eng. 28, 385–414.

Betsh, P., Gruttmann, F., Stein, E., 1996. A 4-node shell element for the implementation of general hyperelastic 3D-elasticity at finite strains. Comput. Meth. Appl. Mech. Eng. 130, 57–79.

Bischoff, M., 1999. Theorie und Numerik einer dreidimensionalen Schalen-formulierung. Institut für Baustatik, Universität Stuttgart, Ber. Nr 30, Stuttgart.

Bischoff, M., Ramm, E., 2000. On the physical significance of higher order kinematic and static variables in a three-dimensional shell formulation. Int. J. Solids Struct. 37, 6933–6960.

Bischoff, M., Wall, W.A., Bletzinger, K.-U., Ramm, E., 2004. Models and finite elements for thin-walled structures. In: Stein, E., de Borst, R., Hughes, T.J.R. (Eds.), Encyclopedia of Computational Mechanics, vol. 2. Wiley, Chicester, pp. 59–137. Chapter 3.

Bolle, L., 1947. Contribution au probléme linéaire de flexion d'une plaque élastique. Bull. Tech. Suisse Rom. 73 (21), 281–285.

Botasso, C.L., Bauchau, O.A., Choi, J.Y., 2002. An energy decaying scheme for nonlinear dynamics of shells. Comput. Meth. Appl. Mech. Eng. 191, 3099–3121.

Cardoso, R.P.R., Yoon, J.W., Mahardika, M., Choudry, S., Alves de Sousa, R.J., Valente, R.A.F., 2008. Enhanced assumed strain (EAS) and assumed natural strain (ANS) methods for one-point quadrature solid-shell elements. Int. J. Numer. Meth. Eng. 75, 156–187.

Chróscielewski, J., Kreja I., Sabik A., Witkowski W., in press. Modeling of composite shells in 6-parameter nonlinear theory with drilling degree of freedom. Mech. Adv. Mater. Struct.

Chróścielewski, J., Makowski, J., Pietraszkiewicz, W., 2002. Non-linear dynamics of flexible shell structures. Comput. Ass. Mech. Eng. Sci. 9, 341–357.

Chróścielewski, J., Makowski, J., Pietraszkiewicz, W., 2004. Statics and Dynamics of Multi-Shells: Nonlinear Theory and Finite Element Method (in Polish). IFTR PASci Press, Warsaw.

Chróścielewski, J., Makowski, J., Stumpf, H., 1992. Genuinely resultant shell finite elements accounting for geometric and material non-linearity. Int. J. Numer. Meth. Eng. 35, 63–94.

Chróścielewski, J., Makowski, J., Stumpf, H., 1997. Finite element analysis of smooth, folded and multi-shell structures. Comput. Meth. Appl. Mech. Eng. 41, 1–46.

Chróścielewski, J., Witkowski, W., 2006. Four-node semi-EAS element in six-field nonlinear theory of shells. Int. J. Numer. Meth. Eng. 68, 1137–1179.

Chróścielewski, J., Witkowski, W., 2010a. On some constitutive equations for micropolar plates. Z. Angew. Math. Mech. 90 (1), 53–64.

Chróścielewski, J., Witkowski, W., 2010b. Discrepancies of energy values in dynamics of three intersecting plates. Int. J. Numer. Meth. Biomed. Engng. 26, 1188–1202. doi:10.1002/cnm.1208.

Eberlein, R., Wriggers, P., 1999. Finite element concepts for finite elastoplastic strain and isotropic stress response in shells: theoretical and computational analysis. Comput. Meth. Appl. Mech. Eng. 171, 243–279.

Eremeyev, V.A., Pietraszkiewicz, W., 2004. The non-linear theory of elastic shells with phase transitions. J. Elasticity 74, 67–86.

Eremeyev, V.A., Pietraszkiewicz, W., 2006. Local symmetry group in the general theory of elastic shells. J. Elasticity 85, 125–152.

Eremeyev, V.A., Pietraszkiewicz, W., 2009. Phase transitions in thermoelastic and thermoviscoelastic shells. Arch. Mech. 61 (1), 41–67.

Eremeyev, V.A., Zubov, L.M., 2008. Mechanics of Elastic Shells (in Russian). Nauka, Moscow.

Green, A.E., Naghdi, P.M., Wenner, M.L., 1971. Linear theory of Cosserat surface and elastic plates of variable thickness. Proc. Camb. Phil. Soc. 69, 227–254.

Green, A.E., Zerna, W., 1968. Theoretical Elasticity, second ed. Clarendon Press, Oxford.

Grigoljuk, E.I., Selezov, I.T., 1973. Non-classical theories of vibrations of bars, plates, and shells. In: Summaries of Science and Technology. Mechanics of Deformable Solids, vol. 5. VINITI, Moscow, pp. 1–273 (in Russian).

Gurtin, M.E., 1972. The linear theory of elasticity. In: Truesdell, C. (Ed.), Handbuch der Physik, Band VIa/2. Springer, Berlin, pp. 1–295.

Ibrahimbegović, A., 1997. Stress resultant geometrically exact shell theory for finite rotations and its finite element implementation. Appl. Mech. Rev. 50 (4), 199–226.

Ibrahimbegović, A., Frey, F., 1994. Stress resultant geometrically nonlinear shell theory with drilling rotations – part II: computational aspects. Comput. Meth. Appl. Mech. Eng. 118, 285–308.

Jemielita, G., 2001. The shear correction factor k. In: Woźniak, C. (Ed.), Mechanics of Elastic Shells and Plates. Polish Scientific Publishing House, pp. 136–149 (in Polish; Chapter II.9).

John, F., 1965. Estimates for the derivatives of the stresses in a thin shell and interior shell equations. Commun. Pur. Appl. Math. 18 (1), 235–267.

Kleiber, M., Woźniak, Cz., 1991. Nonlinear Mechanics of Structures. PWN, Warszawa.

Kuhl, D., Ramm, E., 1996. Constraint energy momentum algorithm and its application to non-linear dynamics of shells. Comput. Meth. Appl. Mech. Eng. 136, 293–315.

Lee, H.P., Haris, P.J., 1979. Post-buckling strength of thin-walled members. Comput. Struct. 10, 689–702.

Libai, A., Simmonds, J.G., 1983. Nonlinear elastic shell theory. Adv. Appl. Mech. 23, 271–371.

Libai, A., Simmonds, J.G., 1998. The Nonlinear Theory of Elastic Shells, second ed. Cambridge University Press, Cambridge, UK.

Lubowiecka, I., Chróścielewski, J., 2005. Energy-conserving time integration algorithm for six-field irregular shell dynamics. In: ECCOMAS Thematic Conference: Advances in Computational Multibody Dynamics: Proceedings of Multibody Dynamics 2005, Madrid, 21–24, June 2005, ETS Ingenieros de Caminos Canales y Puertos, Universidad Politecnica de Madrid, Madrid, pp. 1–16.

Lubowiecka, I., Chróścielewski, J., 2002. On dynamics of flexible branched shell structures undergoing large overall motion using finite elements. Comput. Struct. 80, 891–898.

MacNeal, R.H., Harder, R.L., 1985. A proposed standard set of problems to test finite element accuracy. Finite Elem. Anal. Des. 1, 3–20.

Miehe, C., Shroeder, J., 2001. Energy and momentum conserving elastodynamics of non-linear brick-type mixed finite shell element. Int. J. Numer. Meth. Eng. 50, 1801–1823.

Naghdi, P.M., 1963. Foundations of elastic shell theory. In: Sneddon, I.N., Hill, R. (Eds.), Progress in Solid Mechanics, vol. 4. North-Holland Publishing Company, Amsterdam, pp. 1–90.

Naghdi, P.M., 1972. The theory of shells and plates. In: Handbuch der Physik, Band VIa/2. Springer-Verlag, Berlin, pp. 425–640.

Noor, A.K., Burton, W.S., 1989. Assessment of shear deformation theories for multilayered composite plates. Appl. Mech. Rev. 42 (1), 1–13.

Owen, D.R.J., Hinton, E., 1980. Finite Elements in Plasticity: Theory and Practice. Pineridge Press, Swansea, UK.

Panasz, P., Wiśniewski, K., 2008. Nine-node shell elements with 6 dofs/node based on two-level approximations. Part I theory and linear tests. Finite Elem. Anal. Des. 44, 784–796.

Pietraszkiewicz, W., 1979a. Consistent second approximation to the elastic strain energy of a shell. ZAMM 59, 206–208.

Pietraszkiewicz, W., 1979b. Finite Rotations and Lagrangean Description in the Non-Linear Theory of Shells. Polish Scientific Publishers, Warsaw, Poznań.

Pietraszkiewicz, W., Badur, J., 1983. Finite rotations in the description of continuum deformation. Int. J. Eng. Sci. 21 (9), 1097–1115.

Reissner, E., 1944. On the theory of bending of elastic plates. J. Math. Phys. 23, 184–191.

Reissner, E., 1974. Linear and nonlinear theory of shells. In: Thin Shell Structures. Prentice-Hall, Englewood Cliffs, NJ, pp. 29–44.

Rubin, M.B., 2000. Cosserat Theories: Shells, Cods, and Points. Kluwer Academic Publishers, Dordrecht.

Simo, J.C., Fox, D.D., 1989. On a stress resultant geometrically exact shell model. Part I: Formulation and optimal parameterization. Comput. Meth. Appl. Mech. Eng. 72, 267–304.

Simo, J.C., Tarnow, N., 1994. A new energy and momentum conserving algorithm for the non-linear dynamics of shells. Int. J. Numer. Meth. Eng. 37, 2527–2549.

Simo, J.C., Vu-Quoc, L., 1988. On the dynamics in space of rods undergoing large motions. A geometrically exact approach. Comput. Meth. Appl. Mech. Eng. 66, 125–161.

Tan, X.G., Vu-Quoc, L., 2005. Efficient and accurate multilayer solid/shell element: nonlinear materials at finite strain. Int. J. Numer. Meth. Eng. 63, 2124–2170.

Vu-Quoc, L., 1986. Dynamics of Flexible Structures Performing Large Overall Motions: Geometrically Nonlinear Approach, PhD Dissertation, ERL Memorandum UCB/ERL M86/36, UC Berkeley.

Vu-Quoc, L., Deng, H., Tan, X.G., 2000. Geometrically exact sandwich shells: the static case. Comput. Meth. Appl. Mech. Eng. 189, 167–203.

Vu-Quoc, L., Deng, H., Tan, X.G., 2001. Geometrically exact sandwich shells: the dynamic case. Comput. Meth. Appl. Mech. Eng. 190, 2825–2873.

Vu-Quoc, L., Ebcioglu, I.K., 2000. Multilayer shells: geometrically exact formulation of equations of motion. Int. J. Solids Struct. 37, 6705–6737.

Vu-Quoc, L., Ebcioglu, I.K., 2005. On the physical meaning of the dynamical equations governing geometrically exact multilayer shells. Comput. Meth. Appl. Mech. Eng. 194, 2363–2384.

Vu-Quoc, L., Tan, X.G., 2003. Optimal solid shells for nonlinear analyses of multilayer composites. Part II: dynamics. Comput. Meth. Appl. Mech. Eng. 192, 1017–1059.

Wagner, W., Gruttmann, F., 2005. A robust non-linear mixed hybrid quadrilateral shell element. Int. J. Numer. Meth. Eng. 64, 635–666. doi:10.1002/nme.1387.

Yeh, J.T., Chen, W.H., 1993. Shell elements with drilling degree of freedoms based on micropolar elasticity theory. Int. J. Numer. Meth. Eng. 36, 1145–1159.

Zhong, H.G., Crisfield, M.A., 1998. An energy-conserving co-rotational procedure for the dynamics of shell structures. Eng. Comput. 15, 552–576.